

A Calibrated Data-Driven Approach for Small Area Estimation using Big Data

Siu-Ming Tam¹ and Shaila Sharmeen²

¹National Institute of Applied Statistical Research, University of Wollongong, Northfields Avenue, Wollongong, NSW 2522, Australia and Methodology and Data Science Division, Australian Bureau of Statistics, ABS House, Benjamin Way, Belconnen 2617, Australia. Email: stattam@gmail.com.

²School of Information Technology, Deakin University, Burwood, Vic 3125, Australia. Email: shailacse2k@gmail.com.

Abstract

Where the response variable in a big data set is consistent with the variable of interest for small area estimation, the big data by itself can provide the estimates for small areas. These estimates are often subject to the coverage and measurement error bias inherited from the big data. However, if a probability survey of the same variable of interest is available, the survey data can be used as a training data set to develop an algorithm to impute for the data missed by the big data and adjust for measurement errors. In this paper, we outline a methodology for such imputations based on an kNN algorithm calibrated to an asymptotically design-unbiased estimate of the national total, and illustrate the use of a training data set to estimate the imputation bias and the “fixed - k asymptotic” bootstrap to estimate the variance of the small area hybrid estimator. We illustrate the methodology of this paper using a public use data set and use it to compare the accuracy and precision of our hybrid estimator with the Fay-Harriot (FH) estimator. Finally, we also examine numerically the accuracy and precision of the FH estimator when the auxiliary variables used in the linking models are subject to under-coverage errors.

Keywords: Calibration; CkNN algorithm; Fixed - k asymptotic bootstrap; Hybrid estimation. Imputation bias.

1 INTRODUCTION

In official statistics, there is generally a significant, but often unmet, growing demand for small area statistics for decision making at the local level. By small area, we mean small geographical parcels of land where direct estimates from surveys generally fail to provide reliable estimates. Direct estimates fail because the sample size from probability surveys for the small areas is either too small or zero, i.e. there is no sample available for them, for reliable estimation. As a result, the “design-based approach” that is commonly adopted in official statistical surveys invariably fail to deliver good small area estimates (SAE). To overcome this problem, survey statisticians appeal to a “model-based approach” and use statistical models to “borrow strength” across areas (Fay and Herriot, 1979; Battese et al. 1988), across time (Pfeffermann and Tiller, 2006), or resort to synthetic estimation (Lehtonen and Veiganen, 2009). For a comprehensive account of the small area estimation methods, refer to Datta (2009), Ghosh and Rao (1994), Ghosh (2020), Jiang and Lahiri (2006a, 2006b), Pfeffermann (2002, 2013), Rao (2005, 2008) and Rao and Molina (2015).

With more and more data captured through the “internet of things (IoT)” - a system of interrelated computing devices, mechanical and digital machines, objects, animals or people that are provided

with unique identifiers and the ability to transfer data over a network without requiring human-to-human or human-to-computer interaction (Daas et al., 2015; Tam and Clarke, 2015, Wiki, 2022) - what are the opportunities for SAE through borrowing strength from additional data sources? Whilst excellent attempts have been made in the literature to harness the information from the big data set, current research appears to be using the big data as a source for auxiliary variables in SAE unit level models (Battese et. al., 1988), or SAE area level models (Beaumout, 2020; Marchetti et al., 2015; Porter et al., 2014; Schmid et al., 2017; Rao, 2021). It is well known that many types of big data suffer from representational and measurement errors (Amaya et al., 2020), the use of big data as auxiliary variables in the Fay and Herriot (FH) model can lead to estimates which are worse than direct estimates (Ybarra and Lohr, 2008). Using a measurement error model, Ybarra and Lohr (2008) proposed a modified FH estimator by adjusting the weights of the convex combination of the direct estimate and model estimate of the small area, to address measurement errors in the auxiliary variables.

In this paper, we advocate a different approach to SAE by borrowing strength from big data. What is big data? According to the Big Data Privacy Report (Podesta *et al.*, 2014), the definition of big data depends on one's perspective - '... there are many definitions of Big Data, which differ on whether you are a computer scientist, a financial analyst, or an entrepreneur pitching an idea to a venture capitalist.....'. The characteristics of big data have been popularly defined by five V's in the ICT literature, namely, Volume, Velocity, Variety, Veracity and Vulnerability. All of these do not actually define what big data is. Tam and van Halderen (2020) defined big data as the collection of the data from classical and IoT sources, and provided a schematic representation of the types of big data that may be useful to compile official statistics.

To illustrate ideas, we shall henceforth assume that there are no measurement errors in the big data, nor data linking errors between the big data and the probability survey data. The former issue was addressed in Tam et. al. (2020) and the latter in Kim and Tam (2021), and we shall not repeat their arguments here.

By considering the small area as comprising two strata, the big data stratum and a missing data stratum, the estimate for the small area is then the sum of the observed total of the variable of interest in the big data stratum and the estimated total in the missing data stratum. How do we estimate the total of the missing data stratum? If we have imputed values of the missing data, the total is then the sum of these imputed values. Imputing the missing values *en masse* is often referred to as mass imputation (Chipperfield et al., 2012). How do we impute? We can resort to classical methods (see, for example, Kim et. al., 2020) or machine learning algorithms. In this paper, we use a k-Nearest Neighbours (kNN) algorithm (Hastie and Tibshirani, p 463, 2008), but with the sum of the observed and imputed values calibrated to an approximately unbiased estimate - referred to as data integrator in Kim and Tam (2021) - of the population total at the national level. We call the resultant estimate as a hybrid estimate and the method hybrid estimation. The use of such calibration approach is not new - see for example, Beaumont (2005). Because the imputed values do not necessarily equal to the true but unobserved values, an imputation bias of the small area estimator is expected. Using the sample in the missing data stratum, we can estimate the imputation bias. Also inspired by the fixed - k asymptotic method (Otsu and Rai, 2017) to bootstrap (Effron and Tibshirani, p. 124, 1986), we can estimate the variance of the hybrid estimator and thus its mean squared error to make inference on the small area total. Where the variable of interest in the big data is subject to measurement error, we can remove it using either a deterministic method if there is a priori information on the systematic nature of the error, or statistical modelling if the error is random. For the rest of the paper, we assume that the variable of interest is measured without error in both the big data and probability survey data sets.

The layout of the paper is as follows. The notation will be introduced and some well-known results are presented in Section 2. The methodology for SAE using big data and kNN subject to calibration – hereinafter referred to as a calibrated kNN algorithm (CkNN), imputation bias and confidence interval estimation will be described in Section 3. Section 4 gives an application of the methodology to a population data set from the Australian Bureau of Statistics and reports the comparison of the CkNN small area estimates with the FH estimates. It also examines the quality of the FH estimates when the auxiliary variables derived from big data are subject to coverage error. Finally, we conclude in Section 5.

2 NOTATIONS AND AN ESTABLISHED RESULT

Suppose we have a finite population, $U = \{1, \dots, N\}$ comprising N units with the following values, x_i and $y_i, \forall i \in U$, where x_i is a vector of auxiliary variables and is fully observed, and y_i is the variable of interest. We assume that $U = B \cup C$, where B , of size N_B , comprises the labels of the big data set and C , of size N_C , is the complement of B . We assume further that $y_i, \forall i \in B$, are observed without error. Finally, we also assume that we have a probability sample, $A \subset U$, with known design weights of the sample, $d_i, \forall i \in A$. Thus we have the following data available to the analyst for SAE: (a) (x_i, y_i) for $i \in B$; (b) (d_i, x_i, y_i) for $i \in A$; (c) $x_i, \forall i \in C$ and (d) information on where these units are located in the small area. Finally, let δ_i denote the big data inclusion indicator which is 1 if unit $i \in B$ and 0 otherwise. We assume that (e) $\delta_i, \forall i \in A$, is fully observed. Note that $\delta_i = 1$ is observed for $\forall i \in B$. In addition, note that the case when A is subject to nonresponse and δ_i not fully observed was addressed in Tam et al (2020) and Kim and Tam (2021) respectively and will not be repeated here.

Suppose further that $U = U_1 \cup \dots \cup U_m \cup \dots \cup U_M, B = B_1 \cup \dots \cup B_m \cup \dots \cup B_M$ and $C = C_1 \cup \dots \cup C_m \cup \dots \cup C_M$ and $A = A_1 \cup \dots \cup A_m \cup \dots \cup A_M$, where $U_m = B_m \cup C_m$ and m denotes the m^{th} small area. For SAE, we are interested to estimate $T_m = \sum_{i \in U_m} y_i, m = 1, \dots, M$. As

$T_m = \sum_{i \in B_m} y_i + \sum_{i \in A_m \setminus B_m} y_i + \sum_{i \in C_m \setminus A_m} y_i = T_{B_m} + T_{A_m \setminus B_m} + T_{C_m \setminus A_m}$, and because T_{B_m} and $T_{A_m \setminus B_m}$ are fully observed, the SAE problem boils down to estimating $T_{C_m \setminus A_m}$, using the information available from (a) to (e) above.

Denote the population total by $T = \sum_{m=1}^M T_m$. Kim and Tam (2021) showed that the data integrator,

perhaps better referred to as a hybrid estimator, $\hat{T}_P = \sum_{i \in U} \delta_i y_i + N_C \frac{\sum_{i \in A} d_i (1 - \delta_i) y_i}{\sum_{i \in A} d_i (1 - \delta_i)}$, is equivalent to a

generalised regression estimators and hence is approximately designed unbiased (Särndal et. al.,

1992, p 235). For simple random sampling of size n , $Var(\hat{T}_p) \approx (1 - W_B) \frac{N^2}{n} S_C^2$, where

$W_B = N_B / N$, $n / N \approx 0$, $S_C^2 = N_C^{-1} \sum_1^N (1 - \delta_i)(y_i - \bar{Y}_C)^2$ and $\bar{Y}_C = N_C^{-1} \sum_1^N (1 - \delta_i)y_i$. Furthermore,

if $S^2 = N^{-1} \sum_1^N (y_i - \bar{Y})^2$ and $\hat{T}_A = N \sum_{i \in A} y_i / n$, Kim and Tam (2021) showed that

$\frac{Var(\hat{T}_p)}{Var(\hat{T}_A)} = (1 - W_B) \frac{S_C^2}{S^2} < 1$, if $(1 - W_B)S_C^2 < S^2$. In other words, when W_B is sufficiently large or

$S_C^2 \approx S^2$, \hat{T}_p is a more efficient estimator than \hat{T}_A . As \hat{T}_p is an efficient estimator of the population total, we use it as the constraint to mass impute the missing values in $C \setminus A$.

3 METHODOLOGY FOR SAE WITH BIG DATA

Let \hat{y}_i denote the imputed value of the missing data for unit $i \in C$. We want the imputed values to satisfy the following conditions:

- (a) $\hat{y}_i = y_i$ if $i \in D$ where $D = A \cap C$; and
- (b) $\hat{T}_C = \hat{T}_p - T_B$, where $\hat{T}_C = \sum_{i \in C} \hat{y}_i$ and $T_B = \sum_{i \in B} y_i$.

Provided that such an imputation methodology is developed, we can estimate T_m by

$\hat{T}_m = T_{B_m} + \hat{T}_{C_m} = T_{B_m} + \sum_{i \in C_m} \hat{y}_i$. Here, \hat{T}_m can be considered as a synthetic SAE. From (b),

$\hat{T} = \sum_{m=1}^M \hat{T}_m = \sum_{m=1}^M (T_{B_m} + \hat{T}_{C_m}) = \hat{T}_p$. Subjecting small area estimates to constraints is not a new concept,

see, for example, Pfeffermann and Tiller (2006). In their paper, the constraint is used to provide protection against possible model failure. In this paper, the constraint is imposed to ensure that the sum of small area estimates equals to the efficient and approximately unbiased estimator of the national population total, \hat{T}_p , to ensure consistency between the sum of the SAEs and national total. This approach is also used in Beaumont (2005).

3.1 DEVELOPING THE CALIBRATED kNN (CkNN) ALGORITHM

Because $D = A \cap C$ is a probability sample of C , i.e. each unit in C has a known and non-zero probability of inclusion in D , the MAR assumption and positivity assumptions to justify the use of kNN (Yang and Kim, 2019) are satisfied. Let $D = D_1 \cup \dots \cup D_m \cup \dots \cup D_M$ and $|D_m| = n_{D_m}$ where n_{D_m} is

known. We introduce a second subscript m to denote the small area in which the training data point is located, e.g. y_{mi} denotes that the data point i is located in small area m .

For the kNN algorithm, there are two hyper-parameters to be estimated, namely, the number of nearest neighbours, k , and number and nature of the features, $p = \dim(\mathbf{x}_i)$ to be determined using “feature engineering” as so described in data science or variables selection in statistics.

Mathematically, we want to find the optimum k and p such that sum over M of the absolute prediction error in each small area is a minimum. If \hat{y}_{mi} (which depends on \mathbf{x}_{mi}, k, p) denotes the predicted value of y_{mi} , $L(\hat{y}_{mi}, y_{mi}) = \hat{y}_{mi} - y_{mi}$, denotes the “loss function” being defined here as the

prediction error for the data point, the prediction error for the m^{th} small area is $\sum_{i=1}^{n_m} (\hat{y}_{mi} - y_{mi})$,

where $|C_m \setminus A_m| = n_{C_m \setminus A_m}$.

Following Wesley et al (2022) and Hastie et al (2008, p. 181), we use K-fold cross validation applied to the training data set D , to determine k and p , which are to be solutions to minimise the following objective function:

$$\arg \min_{k,p} \left\{ \frac{1}{n_D} \sum_{j=1}^K \sum_{m=1}^M \left| \sum_{mi: \rho(mi)=j} L(y_{mi}, f^{-j}(\mathbf{x}_{mi}, k, p)) \right| \right\} \quad (1)$$

where n_D is the sample size of D ; $\hat{y}_{mi} = f^{-j}(\mathbf{x}_{mi}, k, p)$ is the kNN predictor of y_{mi} , given the auxiliary vector, \mathbf{x}_{mi} , k and p based on the data from D less the j^{th} fold; and

$\rho: \{1, \dots, n_D\} \mapsto \{1, \dots, K\}$ is the indexing function that indicates the fold to which observation indexed by mi is allocated by a randomization process in such a way that the folds are as far as possible equal in size, so that the third summation sign in (1) denotes the summation over those mi 's in the

j^{th} fold. The objective function $\left\{ \frac{1}{n_D} \sum_{j=1}^K \sum_{m=1}^M \left| \sum_{mi: \rho(mi)=j} L(y_{mi}, f^{-j}(\mathbf{x}_{mi}, k, p)) \right| \right\}$ is referred to as the

estimated test error rate (Hastie et al, p. 181, 2008) from the training data set. Note that we want

the kNN algorithm trained to minimise $\sum_{m=1}^M \sum_{i=1}^{n_{J_m}} (\hat{y}_{mi} - y_{mi})$ rather than $\sum_{m=1}^M \sum_{i=1}^{n_{J_m}} |\hat{y}_{mi} - y_{mi}|$ for SAE, where

$n_{J_m} = |J_m|$ and J_m represents the m^{th} small area in the fold. This is because we want to minimise the prediction error in all of the small areas, and do not want the error in one area to be offset by the errors of other areas. This will be an appropriate objective function as long as we are interested in getting the predicted counts in the small areas as close as possible to the actual count, and not accuracy in the individual predicted values, in which case, the objective function would be

$$\sum_{m=1}^M \sum_{i=1}^{n_{J_m}} |\hat{y}_{mi} - y_{mi}|.$$

What distance metric should be used to find the nearest neighbours? Alfeilat et al. (2019) gave a comprehensive review and evaluation of the distance metrics that may be used in kNN algorithms and concluded that the Hassanat Distance (HasD) metric (Hassanat, 2014) performs the best when applied to a diversity of data sets. The HasD, which is used in the application in Section 4 below,

between the points $\mathbf{x}_i = (x_{i1}, \dots, x_{ip})^T$ and $\mathbf{x}_j = (x_{j1}, \dots, x_{jp})^T$, is defined as follows:

$$\text{HasD}(\mathbf{x}_i, \mathbf{x}_j) = \frac{1}{p} \sum_{l=1}^p D(x_{il}, x_{jl}) \text{ where for } l=1, \dots, p, \text{ and } x_{il} \text{ or } x_{jl} \neq 0$$

$$D(x_{il}, x_{jl}) = 1 - \frac{1 + \min(x_{il}, x_{jl})}{1 + \max(x_{il}, x_{jl})}, \text{ if } \min(x_{il}, x_{jl}) \geq 0; \text{ or } 1 - \frac{1 + \min(x_{il}, x_{jl}) + |\min(x_{il}, x_{jl})|}{1 + \max(x_{il}, x_{jl}) + |\min(x_{il}, x_{jl})|} \text{ otherwise.}$$

Where $x_{il} = x_{jl} = 0$, we define $D(x_{il}, x_{jl}) = 0$. Furthermore, Hassanat (2014) showed that $D(x_{il}, x_{jl})$ is bounded between 0 (when $x_{il} = x_{jl} \forall l = 1, \dots, p$) and 1 (when the distance x_{il} and x_{jl} is infinite for one $l = 1, \dots, p$); symmetric (i.e. $D(x_{il}, x_{jl}) = D(x_{jl}, x_{il})$) and satisfies the triangular inequality (i.e.

$$D(x_{il}, x_{jl}) \leq D(x_{il}, x_{kl}) + D(x_{kl}, x_{jl}).$$

Under kNN, the predictor (i.e. imputed value) is the arithmetic average of the k nearest neighbours, i.e. the weight attached to each of the nearest neighbours is the same $\frac{1}{k}$. In other words, if

$\{y_{i(1)}, \dots, y_{i(j)}, \dots, y_{i(k)}\}$ is the set of the k nearest neighbours of $i \in C \setminus D$ as determined by HasD,

the kNN predictor is $\sum_{j=1}^k \frac{y_{i(j)}}{k}$. Instead of using an arithmetic average of the k nearest neighbours,

we use a convex weighted average so as to ensure that the imputed values satisfy the calibration property (see (a) and (b) in the Lemma below), and want the weights, $w_j, j = 1, \dots, k$, to be chosen as

close to $\frac{1}{k}$ as possible. We use the Chi-square distance of Deville and Sarndal (1992) to determine

closeness, i.e. $\sum_{j=1}^k k(w_j - \frac{1}{k})^2$.

Lemma. The solution to $\arg \min_{w_j} \sum_{j=1}^k \frac{1}{k} (kw_j - 1)^2$ subject the following constraints:

a. $\sum_{i \in C} \hat{y}_i = \hat{T}_p - T_B = \hat{T}_C$, where $\hat{y}_i = y_i$ for $i \in D$, and $\hat{y}_i = \sum_{j=1}^k w_j y_{i(j)}$ for $i \in C \setminus D$; and

b. $\sum_{j=1}^k w_j = 1$

is:

$$w_j = \frac{1}{k} + \frac{\left\{ \hat{T}^{(j)} - \frac{1}{k} \sum_{j=1}^k \hat{T}^{(j)} \right\}}{\left\{ \sum_{j=1}^k (\hat{T}^{(j)})^2 - \frac{1}{k} (\sum_{j=1}^k \hat{T}^{(j)})^2 \right\}} (\hat{T}_p - \hat{T}_{kNN}) \quad (2)$$

where $\hat{T}^{(j)} = \sum_{i \in C \setminus D} y_{i(j)}$, $j = 1, \dots, k$, $\hat{T}_{kNN} = T_B + T_D + \frac{1}{k} \sum_{j=1}^k \hat{T}^{(j)}$, and $T_D = \sum_{i \in D} y_i$. Thus

$$\hat{T}_{CkNN} = T_B + T_D + \sum_{j=1}^k w_j \hat{T}^{(j)}, \text{ where } w_j \text{ is given by (2).}$$

Proof

The constraint in (a) can be rewritten as $\hat{T}_C - T_D = \sum_{i \in C \setminus D} \sum_{j=1}^k w_j y_{i(j)} = \sum_{j=1}^k w_j \hat{T}^{(j)}$. Using Lagrange

Multipliers, $2\lambda_1$ for (1) and $2\lambda_2$ for (b), differentiating $\sum_{j=1}^k k(w_j - \frac{1}{k})^2 = \sum_{j=1}^k \frac{1}{k}(kw_j - 1)^2$ and

simplifying, we have:

$$w_j = \frac{1}{k} + \frac{\lambda_1 \hat{T}^{(j)}}{k} + \frac{\lambda_2}{k}. \quad (3)$$

Using $\hat{T}_C - T_D = \sum_{j=1}^k w_j \hat{T}^{(j)}$ and $1 = \sum_{j=1}^k w_j$, we get:

$$\hat{T}_C - T_D = \frac{1}{k} \sum_{j=1}^k \hat{T}^{(j)} + \frac{\lambda_1}{k} \sum_{j=1}^k (\hat{T}^{(j)})^2 + \frac{\lambda_2}{k} \sum_{j=1}^k \hat{T}^{(j)}; \text{ and } \frac{\lambda_1}{k} \sum_{j=1}^k \hat{T}^{(j)} + \lambda_2 = 0. \text{ Solving and putting:}$$

$$\lambda_1 = \frac{k(\hat{T}_C - T_D - \frac{1}{k} \sum_{j=1}^k \hat{T}^{(j)})}{\left\{ \sum_{j=1}^k (\hat{T}^{(j)})^2 - \frac{1}{k} (\sum_{j=1}^k \hat{T}^{(j)})^2 \right\}} = \frac{k(\hat{T}_p - \hat{T}_{kNN})}{\left\{ \sum_{j=1}^k (\hat{T}^{(j)})^2 - \frac{1}{k} (\sum_{j=1}^k \hat{T}^{(j)})^2 \right\}},$$

and $\lambda_2 = -\frac{\lambda_1}{k} \sum_{j=1}^k \hat{T}^{(j)}$ into (3), the required result (2) is obtained.

We note that the first condition of the Lemma ensures that $\hat{T}_C + T_B$ is calibrated to the data integrator, \hat{T}_p , of Kim and Tam (2021).

3.2 SMALL AREA ESTIMATORS WITH CkNN

It follows from the Lemma that the CkNN, or hybrid, estimator of the population total is given by:

$$\begin{aligned} \hat{T}_{CkNN} &= \hat{T}_p \\ &= T_B + T_D + \sum_{j=1}^k w_j \hat{T}^{(j)} \\ &= T_B + T_D + \sum_{j=1}^k w_j \left(\sum_{i \in C \setminus D} y_{i(j)} \right) \\ &= T_B + T_D + \sum_{i \in C \setminus D} \left(\sum_{j=1}^k w_j y_{i(j)} \right) \end{aligned}$$

from which, the calibrated kNN small area estimator for small area m is given by:

$$\hat{T}_{CkNN_m} = T_{B_m} + T_{D_m} + \sum_{i \in C_m \setminus D_m} \left(\sum_{j=1}^k w_j y_{i(j)} \right). \text{ To simplify notations, we will use } \hat{T}_m \text{ to represent } \hat{T}_{CkNN_m} \text{ and } \hat{T}_{C_m \setminus D_m} \text{ to represent } \sum_{i \in C_m \setminus D_m} \left(\sum_{j=1}^k w_j y_{i(j)} \right) \text{ in the sequel.}$$

3.3 MEAN SQUARED ERROR FOR \hat{T}_m

From $\hat{T}_m = T_{B_m} + T_{D_m} + \hat{T}_{C_m \setminus D_m}$ and $T_m = T_{B_m} + T_{D_m} + T_{C_m \setminus D_m}$, we have

$$\begin{aligned} \hat{T}_m - T_m &= \hat{T}_{C_m \setminus D_m} - T_{C_m \setminus D_m} \\ &= \left\{ \hat{T}_{C_m \setminus D_m} - E(\hat{T}_{C_m \setminus D_m}) \right\} + \left\{ E(\hat{T}_{C_m \setminus D_m}) - T_{C_m \setminus D_m} \right\} \end{aligned}$$

and, decomposing mean squared errors into variance and bias squared, we have

$$\begin{aligned} MSE(\hat{T}_m) &= E(\hat{T}_m - T_m)^2 \\ &= E \left\{ \hat{T}_{C_m \setminus D_m} - E(\hat{T}_{C_m \setminus D_m}) \right\}^2 + \left\{ E(\hat{T}_{C_m \setminus D_m}) - T_{C_m \setminus D_m} \right\}^2 \\ &= E \left\{ \hat{T}_{C_m \setminus D_m} - E(\hat{T}_{C_m \setminus D_m}) \right\}^2 + E^2(\hat{T}_{C_m \setminus D_m}) e_m^2 \end{aligned}$$

where $e_m = \left\{ E(\hat{T}_{C_m \setminus D_m}) - T_{C_m \setminus D_m} \right\} / E(\hat{T}_{C_m \setminus D_m})$. The error, $E(\hat{T}_{C_m \setminus D_m}) - T_{C_m \setminus D_m}$, is due to the use of nearest neighbours to impute the missing values in $C_m \setminus D_m$ and is the imputation bias. We may describe e_m as the relative imputation bias.

As the unobserved $E(\hat{T}_{C_m \setminus D_m})$, $Var(\hat{T}_m)$ and e_m are functions of kNNs, it is intractable to give a closed form for them. For the first two quantities, the bootstrap offers an attractive technique to provide the estimates. However, Abadie & Imbens (2008) has shown that the “naïve” bootstrap (Efron and Gong, 1983) does not work for kNN problems. This is because the naïve bootstrap does not preserve the distribution of the number of times, denoted by $K_k(i)$, the unit $i \in D$, is used as a donor for imputing the missing values in $C \setminus D$. It is easily seen that $K_k(i)$ changes if bootstraps are drawn from D . To overcome this problem, we use an approach inspired by Otsu and Rai (2017) who use a “fixed - k asymptotic” bootstrap to estimate treatment effects in observational studies based on imputing the “counterfactuals” using kNN, which ensures that $K_k(i)$, $i \in D$, is not altered.

3.3.1 ESTIMATING $E(\hat{T}_{C_m \setminus D_m})$ and $Var(\hat{T}_m)$

It is easy to see that $\hat{T}_{C_m \setminus D_m} = \sum_{i \in A} y_i K_{km}(i)$, where $K_{km}(i) \geq 0$ is defined by $\sum_{j=1}^k n_{km}^{(j)}(i) w_j$ where $n_{km}^{(j)}(i)$ is the number of times y_i is used as the j^{th} nearest neighbour for all the missing data points in

$C_m \setminus D_m$. Because by construction $w_j \approx \frac{1}{k}$, $K_{km}(i) \approx \frac{1}{k} \sum_{j=1}^k n_{km}^{(j)}(i)$. Let $z_{mi} = y_i K_{km}(i) \mid A \mid = n$ and $\psi_m = \{z_{m1}, \dots, z_{mi}, \dots, z_{mm}\}$. The following procedures select “fixed - k asymptotic” bootstraps:

Step 1. Create a bootstrap, ψ_m^* , of the same size n , by sampling ψ_m independently and with replacement.

Step 2. Repeat Step 1 B times to create $\psi_{1m}^*, \dots, \psi_{bm}^*, \dots, \psi_{Bm}^*$, where $\psi_{bm}^* = \{z_{bm1}^*, \dots, z_{bmi}^*, \dots, z_{bmm}^*\}$.

Compute $\hat{T}_{C_m \setminus D_m}^* = \sum_{i=1}^n z_{bmi}^*$ and $\hat{T}_{C_m \setminus D_m} = \frac{1}{B} \sum_{b=1}^B \hat{T}_{C_m \setminus D_m}^*$.

Then $\hat{E}(\hat{T}_{C_m \setminus D_m}) = \hat{T}_{C_m \setminus D_m}$ and $V\hat{a}r(\hat{T}_m) = V\hat{a}r(\hat{T}_{C_m \setminus D_m}) = \frac{1}{B} \sum_{b=1}^B (\hat{T}_{C_m \setminus D_m}^* - \hat{T}_{C_m \setminus D_m})^2$. By treating z_{mi} as

“observations” and resample them, the process is equivalent to resampling from $\{y_{mi}, \mathbf{x}_{mi}, K_{km}(i)\}_{i=1}^n$ (Otsu and Rai, 2017) and hence $K_{km}(i)$ is not altered by the bootstrap process.

How many fixed - k asymptotic bootstraps are required? The bootstrap sample size B is important to determine the accuracy of the end points of the confidence interval. For accelerated

bias correction confidence interval end-points, Efron (1987) shows that, $B \approx \left\{ \frac{1.71}{CV_W} \right\}^2$, where CV_W is

the coefficient of variation of the “width” of the 95% bootstrap confidence interval. It is suggested we use this rule for determining the size of B for variance estimation. For the numerical example below, we set $B=500$, in order to get a CV_W of about 7%.

3.3.2 ESTIMATING e_m

Let \hat{e}_m be an estimator of the relative imputation bias, $e_m = \{E(\hat{T}_{C_m \setminus D_m}) - T_{C_m \setminus D_m}\} / E(\hat{T}_{C_m \setminus D_m})$. Noting that because we know the true value of the target variable in D , we can proceed to estimate e_m as follows:

Step 1. Pick one data point, say y_i from D . Use the HasD metric to find its k nearest neighbours,

$y_{i(1)}, y_{i(2)}, \dots, y_{i(k)}$, from $D \setminus \{y_i\}$. Compute $\hat{y}_i = \sum_{k=i}^K w_k y_{i(k)}$. Create the pair (y_i, \hat{y}_i) .

Step 2. Pick a second data point, y_l from $D \setminus \{y_i\}$, where l is different from previously selected data point(s). Use the HasD metric to find the k nearest neighbours, $y_{l(1)}, y_{l(2)}, \dots, y_{l(k)}$ from $D \setminus \{y_l\}$.

Compute $\hat{y}_l = \sum_{k=i}^K w_k y_{l(k)}$. Create the pair (y_l, \hat{y}_l) .

Step 3. Repeat Step 2 n_{D_m} times to create the sets $\chi_m = \{(y_{mi}, \hat{y}_{mi}) : mi \in D_m\}, m = 1, \dots, M$.

Step 4. Compute an estimate of e_m by $\hat{e}_m = \frac{\sum_{i \in \chi_m} (\hat{y}_{mi} - y_{mi})}{\sum_{i \in \chi_m} \hat{y}_{mi}}$

Thus, the bootstrap estimate of $E^2(\hat{T}_{C_m \setminus D_m})e_m^2$ is given by $\hat{E}^2(\hat{T}_{C_m \setminus D_m})\hat{e}_m^2$.

Step 4 (alternative). When $\sum_{i \in D_m} \hat{y}_{mi}$ (for binary variables) or n_{D_m} (for continuous variables) ≤ 5 , the estimate of e_m becomes unstable. In such situations, compute the alternative estimator of

$$\hat{e}_m \text{ by } \frac{\sum_{m=1}^M \sum_{i \in \chi_m} (\hat{y}_{mi} - y_{mi})}{\sum_{m=1}^M \sum_{i \in \chi_m} \hat{y}_{mi}}.$$

4 AN AUSTRALIAN EXAMPLE

To illustrate our methods, we use the 1% public use micro data file from the 2016 Australian Census (ABS, 2016) (available at <https://www.abs.gov.au/statistics/microdata-tablebuilder/log-your-accounts> to authorised users) to create the population, big data, and the probability sample. Whilst it would be more preferable to use the 100% sample than the 1% sample from the Census, access to the 100% file by researchers is restricted due to privacy considerations. Volunteers are defined in the 2016 Census as people who performed volunteer work for an organisation or group. This consists of help willingly given in the form of time, service or skills, to a club, organisation or association in the twelve months prior to the 2016 Census.

The population, U , has 173,021 personal records. With 56 regions, there is an average of 3,089 personal records per region. Among the 173,021 personal records, there was a total of 35,742 volunteers, giving an overall average volunteer participation rate of about 21%. The number of volunteers ranged between 46 to 1,236 amongst the 56 small areas, and the volunteer participation rate varies between 11% to 31%.

For this example, we are interested to estimate the number of volunteers using both the big data and probability sample for 56 small areas as defined geographically by the Australian Bureau of Statistics.

A simple random sample of 1,730 (i.e. 1% of U) of the personal records was selected to form A . Amongst the 56 areas, the sample size ranges between 3 and 61, with the median at 28, and bottom and top 25% at 21 and 36 respectively. We grouped the small areas into regions, i.e. put contiguous areas together in the same regions such that we have roughly the same number of small areas in all three regions, having regard to Australia's State boundaries. Selection of the big data sample was conducted in the following manner:

- (i) for Region 1, the sample comprised 50% of the volunteer personal records;
- (ii) for Region 2, the sample comprised 50% of the non-volunteer personal records; and
- (iii) for Region 3, the sample was taken randomly from 80% of the personal records.

In addition, we do not keep information on which of the big data records comes from which Region. Hence, mechanism for selecting the big data set is missing-not-at-random. The size of the big data sample using the above sampling scheme has 103,438 personal records (i.e. 60% of U) and 18,548 volunteers (52% of all volunteers). Leaving out the data points in $A \cap C$ which are observed, there are 68,908 data points in $C \setminus A$, to be imputed for volunteers. By comparison, the number of volunteers in A is 341, which ranges between 0 and 14 in A and between 0 and 8 in $A \cap C$ respectively amongst the 56 small areas. Using the method of Kim and Tam (2021), the asymptotically design-unbiased estimate of the total number of volunteers in the population is 36,312. This compares with the actual number of 35,742.

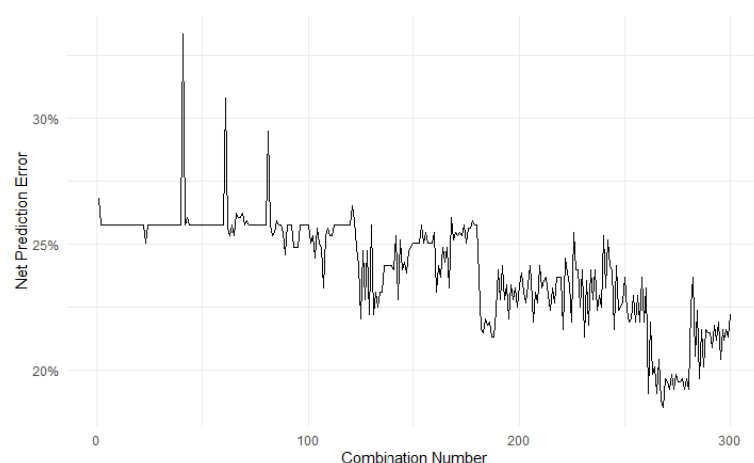
For the CkNN algorithm, we use the following auxiliary variables to find the nearest neighbours: labour force status (employed, unemployed and not in the labour force), birth region (5 groups), age (7 broad groups) and sex (male, female). We also used HasD as the distance metric. Furthermore, we give a value of 1 to a (predicted or actual) volunteer, and 0 otherwise. Thus

$L(y_{mi}, f^{-j(mi)}(x_{mi}, k, p)) = 1$ if $f^{-j(mi)}(x_{mi}, k, p)$ gives a false positive, and $L(y_{mi}, f^{-j(mi)}(x_{mi}, k, p)) = -1$ for a false negative, prediction that the mi^{th} unit is a volunteer. It follows from this definition of the loss function that the test error rate is the average net prediction errors amongst the 56 areas.

To determine the optimum k and p , we used $K=5$ to divide $D=A \cap C$ into 5 folds, and computed the objective function in (1) over all possible combinations (i.e. grid search) of $k=1, \dots, 20$ and $p=1, \dots, 4$ to find the combination with the smallest test error rate. Note that for each p , there are C_p^4 combinations of the four auxiliary variables that may be used for feature selection. Hence the total number of all possible combinations to be tested with is 300.

Figure 1 is a plot of the test error rate against the different combinations of features, p and k . These are presented in the horizontal axis of Figure 1, and description of each combination's features, p and k values are outlined in Appendix 1. It can be seen that the test error rate ranges from 19% to 33%. The lowest test error rate of 19% is achieved using the age, birthplace and labour force status variables, and $k=5$. A test error rate of 19% suggests that the algorithm with this choice of k and the features is expected to be "off" of the national total target by about the same amount. With calibration, however, this off target is substantially reduced, as shown in Table 1 to average at 8.9% across the 56 small areas.

Figure 1: Percentage of net prediction error by different features, p and k



The hybrid estimates of volunteers for the 56 small areas, which we shall denote by \hat{T}_m^{HY} , and their mean squared errors $RTMSE^{HY} = \sqrt{M\hat{SE}(\hat{T}_m^{HY})}$, are provided in the second column and third column respectively in Table 1 in Appendix 2.

The \hat{T}_m^{HY} results in Table 1 are compared with T_m in the upper left graph of Figure 2.

As an indication of the efficacy of the proposed method, we also applied the FH model to estimate the number of volunteers and their mean squared errors, using the same variables used to determine the nearest neighbours. Under the FH formulation, we have the sampling error model and the linking model defined respectively as follows:

Sampling model: $\hat{T}_m^{PR} = T_m + \varepsilon_m$, ε_m is iid and has mean and variance of 0 and σ_m^2 respectively;

Linking model: $T_m = \mathbf{x}_m^T \boldsymbol{\beta} + u_m$, u_m is iid and distributed as $N(0, \sigma_u^2)$

where $\varepsilon_m \perp u_m$ for $m=1, \dots, M$, and where \hat{T}_m^{PR} represents the estimate of T_m using a probability sample, the sampling variance σ_m^2 is assumed known, σ_u^2 and $\boldsymbol{\beta}$ are the (unknown) linking model variance and $p \times 1$ vector of regression coefficients respectively (Fay and Harriot, 1979; Molina and Marhuenda, 2015). Also \mathbf{x}_m is the vector of totals of the same auxiliary variables as those used for computing the HasD metric for the nearest neighbours above, i.e. labour force status (employed, unemployed and not in the labour force), birth region (5 groups), age (7 broad groups) and sex (male, female), for the m^{th} small area. The empirical best linear unbiased predictor for SAE for the m^{th} area is $\hat{T}_m^{FH} = \hat{\gamma}_m \hat{T}_m^{PR} + (1 - \hat{\gamma}_m) \mathbf{x}_m^T \hat{\boldsymbol{\beta}}$,

where $\hat{\gamma}_m = \frac{\hat{\sigma}_u^2}{\hat{\sigma}_u^2 + \sigma_m^2}$ and $\hat{\boldsymbol{\beta}} = \left\{ \sum_{m=1}^M (\hat{\sigma}_u^2 + \sigma_m^2)^{-1} \mathbf{x}_m \mathbf{x}_m^T \right\}^{-1} \left\{ \sum_{m=1}^M (\hat{\sigma}_u^2 + \sigma_m^2)^{-1} \mathbf{x}_m \hat{T}_m^{PR} \right\}$.

The FH estimates together with their MSEs are summarised in the last two columns of Table 1. The calculations were carried out using the R package **saе** and note that normality assumption is not required for point estimation (Molina and Marhuenda, 2015).

The \hat{T}_m^{FH} results in Table 1 are compared with T_m in the upper right graph of Figure 2.

It can be concluded from Figure 2 that the hybrid estimates, \hat{T}_m^{HY} , are more accurate (closer to the diagonal line) and precise (narrow error bands) than the FH estimates, \hat{T}_m^{FH} . Specifically, we can see from Table 1 that the average absolute estimation error (AAER), average relation root mean squared error (ARRTMSE), and coverage rate for the hybrid estimates are 57, 11% and 93% respectively as compared with 107, 28% and 93% respectively for the FH estimates.

In comparing the precision of these estimates, it should be noted that the inference framework for hybrid estimates is designed-based, and for FH estimates model-based.

As the FH model is an area model and given that unit record data is available, we are doing further work to compare estimates from our method with the EBLUP using the unit level model of Battese et. al (1988). We plan to use the data in $B \cup (A \cap C)$ as observed unit data as covariates and a unit-level mixed models (Hobza and Morales, 2016). We hope to publish the results of this research in a future paper.

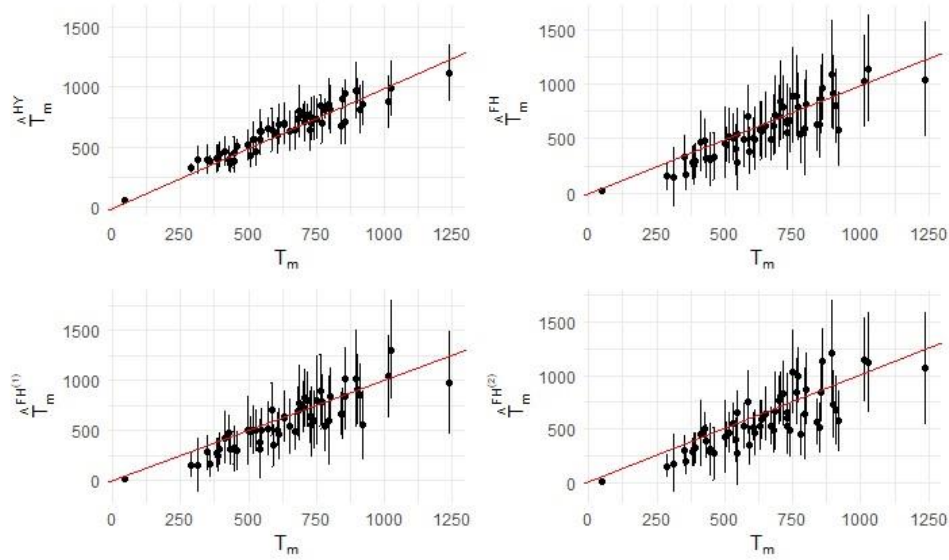
As note earlier, a number of researchers have suggested to use big data directly as auxiliary variables for FH estimation. As far as we are aware, no work has been carried out to date to assess how the differential under-coverage rates in the small areas may affect the FH estimates. To assess this, we have conducted two experiments by artificially creating differential under-coverage rates of the population in the 56 areas by deleting certain number of personal records before re-running the **sae** package. The deletion rates used for these areas are as follows:

Experiment 1 - 5% of the Age1 group records in areas 1- 8 deleted; 10% of the Age2 group records in areas 9-16 deleted; 15% of Age3 group records of the 17-24 area deleted; 20% of Age4 group records in areas 25-32 deleted; 25% of Age5 group records in areas 33 – 40 deleted; 30% of Age6 group records in areas 41-48 deleted and for the rest, 35% of Age 7 group records deleted. The results are denoted by $\hat{T}_m^{FH(1)}$ and $RTM\hat{SE}^{FH(1)} = \sqrt{M\hat{SE}(\hat{T}_m^{FH(1)})}$ in Table 2 in the Appendix.

Experiment 2 - 35%, 40%, 45%, 50%, 55%, 60% and 65% of the records in areas 1- 8, 9-16, 17-24, 25-32 , 33 – 40, 41-48 and 49-56 deleted respectively. The results are denoted by $\hat{T}_m^{FH(2)}$ and $RTM\hat{SE}^{FH(2)} = \sqrt{M\hat{SE}(\hat{T}_m^{FH(2)})}$ in Table 2 in the Appendix.

The data from both experiments are compared against T_m in the lower second two graphs of Figure 2.

Figure 2: Plot of \hat{T}_m , \hat{T}_m^{FH} , $\hat{T}_m^{FH(1)}$, $\hat{T}_m^{FH(2)}$ and their error bars against T_m



Data from Table 1 (upper left and upper right); and data from Table 2 (lower left and left right). Error band is defined as

$$\hat{T}_m' \pm 1.96\sqrt{\widehat{MSE}(\hat{T}_m')} \text{ where } I = HY, FH, FH^{(1)} \text{ or } FH^{(2)}.$$

The lower two graphs of Figure 2 show that the accuracy (as measured by AAER) of the FH estimates is affected to a different extent by the different coverage rate of the auxiliary data. In this numerical example, whilst the reduction in accuracy and precision is marginally affected by incomplete records in the small areas (Experiment 1), it is more significantly affected by incomplete auxiliary information (Experiment 2). This result is in accordance with intuition as there is more information available in Experiment 1 than Experiment 2 for the FH modelling. On the other hand, the estimated coverage rates in both experiments are not statistically significant from the nominal coverage rate of 95% (at 95% confidence).

5. DISCUSSION AND CONCLUSION

This paper outlines a hybrid estimation methodology using calibrated k nearest neighbours for small area estimation. The idea is to borrow strength from big data for SAE. Pre-requisites for the methodology to work are:

- a) the target variables are observed throughout the big data set without measurement errors – this condition is more likely to be satisfied when using administrative data for hybrid estimation than using many other types of big data. Where this condition is not satisfied, $A \cap B$ can be used as a training data set to construct a measurement error model to adjust the target variables in big data (Medous et. al., 2022);

- b) there are no over-coverage errors in the big data. Where this is not the case, $A_m \cap B_m$ can be used to estimate over-coverage rates in the small areas to remove the bias from T_{B_m} ;
- c) the donor set, D , which depends on the size of B and A has to be sufficiently large, to support the imputations. As to what exactly should the size be to make hybrid estimation worthwhile is a topic for further research. In the numerical example, there are 174 donor volunteers out of 675 personal records to support about 69,000 imputations. It is also noted in the numerical example that the imputation bias is the dominant contributing factor of the MSE. This suggests that choice of auxiliary variables and a suitable distance metric for determining the nearest neighbours are also important considerations to minimise the imputation bias;
- d) δ_m is fully observed for the units in A - this can generally be made possible by matching the units between A and B through direct matching or probability matching (Fellegi and Sunter, 1969). When δ_m is not observed, or observed with error, Kim and Tam (2021) developed, using a semi-supervised classification technique, an EM estimator for δ_m ;
- e) associated with each unit of the population, there is a set of covariates which are available and known to the statistician. The assumption presumes the existence of a database with covariates covering the whole of the population. Do such databases exist? They exist (in the form of population registers) in the Scandinavian countries. In New Zealand, a large research database called Integrated Data Infrastructure (IDI) (Statistics New Zealand, 2022) is constructed and maintained using records from government agencies, Statistics New Zealand surveys and non-government organisations. The IDI holds de-identified microdata about people and households in New Zealand and contains such life events information as education, income, benefits, migration, justice and health. In Australia, the multi-agency data integration project (Australian Bureau of Statistics, 2015) created a secure database that integrates records from Australian Bureau of Statistics, Australian Taxation Office, Department of Education, Department of Health and Aged Care, Department of Social Services, Service Australia and Department of Home Affairs. In addition, it is customary for national statistical offices to maintain sampling frames from which probability samples are drawn for business or household surveys. Such sampling frames normally has a limited set of covariates to assist with the selection of optimal samples. For example, business sampling frames generally contain information on the geographic location, industry, employment size in broad categories of businesses; and
- f) the big data set has a target variable of interest to the official statistician, and the national statistics office has a probability survey that collects the same variable, e.g. employment and unemployment data collected from online panels (Callegaro and DiSogra, 2008), and labour force surveys conducted by the national statistics office. The case when the target variable in the big data set suffers from measurement errors has been dealt with in a) above. Integrating data from online panels and probability surveys is the most promising way to construct hybrid estimates.

Note that whilst a calibrated ensemble of machine learning methods may be used in lieu of the

CkNN method of imputation, i.e. $\hat{T}_{EN_m} = T_{B_m} + T_{D_m} + \sum_{j=1}^k w_j \hat{T}_{ML_m}^{(j)}$ where $\hat{T}_{EN} = \sum_{m=1}^M \hat{T}_{EN_m} = \hat{T}_P$ and $\hat{T}_{ML}^{(j)}$

denotes the j^{th} machine learning (ML) method which may be identical with one another but with a different hyper-parameter (e.g. nearest neighbours algorithm, but each ML method differs by their ranking in terms of nearest neighbours) or different in the method itself (e.g. using 1NN for $j = 1$ and support vector machines for $j = 2$ etc.), we prefer to use jNN for the ML algorithm for $j = 1, \dots, k$ because the nearest neighbour methodology has the advantage of minimising the Expected Prediction Error under quadratic loss (Hastie et al, 2008, p. 18).

Using Australian population census data, the CkNN, or hybrid, estimator developed in this paper was compared with FH estimates using an off-the-shelf package and we found that our estimator is on average more accurate and precise than the FH estimator. As noted by a referee, however, the FH estimates in the numerical example are based on an off-the-shelf model but can be improved by, for example, including interactions between the area level covariates in the linking model, or using a binomial likelihood combined with a beta or logit-normal model for the probability of volunteering.

We have also conducted experiments on the accuracy and precision of the FH estimates using auxiliary variables that come from a big data set subject to under-coverage error. The numerical example shows that accuracy of the FH estimates is more affected by under-coverage of personal records in the small areas than by under-coverage of auxiliary variables in the personal records. Ybarra and Lohr (2008) provided methods to adjust for FH estimates when the auxiliary information is subject to sampling variation.

Provided that the pre-requisites underpinning hybrid estimation are satisfied, hybrid estimation, which borrow strength from a suitable big data source, (a) is relatively assumptions free – even though they rely on CkNN to impute the missing values, the variance due to imputation bias can be estimated using a design-based method – and requires less effort to implement e.g. no effort required to develop and test the linking model otherwise required for FH estimation; (b) enables consistency between the sum of SAEs and the national estimate of the variable of interest, thus not undermining confidence in official statistics; (c) through calibration, can render the SAEs to be more accurate than the FH estimates; (d) allows a design-based estimate of the MSE; and (e) is target variable agnostic, i.e. the same algorithm can be applied to target variables of different character. Finally, whilst the CkNN method outlined in this paper looks promising as a design-based estimation method, more work needs to be done to assess its efficacy against EBLUP derived from unit level modelling.

Acknowledgement

We would like to thank an Associate Editor and two referees for their helpful comments on an earlier version of the paper. An earlier version of this paper was presented to the Methodology Advisory Committee of the ABS and we would like to thank the Committee members for their

comments as well. The views expressed in this paper are those of the authors and do not necessarily represent those of the ABS.

APPENDIX 1

The 300 combinations in Figure 1 comprises blocks of 20 combinations each of which consists of $k = 1, \dots, 20$ and one feature below in the following order. E.g. the first combination comprises SEX and $k=1$ and the 20th combination comprises SEX and $k=20$.

Feature details

SEX

Labour Force Status (LFS)

LFS x SEX

Birth Region (BR)

BR x SEX

BR x LFS

BR x LFS x SEX

AGE

AGE x SEX

AGE x LFS

AGE x LFS x SEX

AGE x BR

AGE x BR x SEX

AGE x BR x LFS

AGE x SEX x LFS x BR

APPENDIX 2

Table 1: Estimates for \hat{T}_m , \hat{T}_m^{HY} , $RTM\hat{SE}^{HY}$, \hat{T}_m^{FH} and $RTM\hat{SE}^{FH}$

Small area	T_m	\hat{T}_m^{HY}	$RTM\hat{SE}^{HY}$	\hat{T}_m^{FH}	$RTM\hat{SE}^{FH}$
1	910	811	104	800	176
2	426	401	55	478	105
3	728	641	83	642	141
4	1014	879	111	1029	216
5	839	676*	78	635	127
6	383	404	59	276	80
7	529	468	62	511	112
8	730	741	88	668	174
9	447	387	55	308	129
10	433	364	43	317	95
11	544	630	93	280*	134
12	751	733	87	898	225
13	1236	1119	122	1046	272
14	650	636	87	623	156
15	350	400	62	332	100
16	499	521	64	458	169
17	312	392	58	146	142
18	768	701	88	790	158
19	507	436	52	439	83
20	857	714	91	972	156
21	1026	990	119	1144	252
22	732	698	73	559	173
23	706	708	86	848	187
24	584	646	91	704	148
25	412	462	62	474	142
26	800	813	101	821	156
27	896	968	121	1098	253
28	794	859	110	594	226
29	391	438	56	294	82
30	607	596	76	502	95
31	632	698	90	583	128
32	543	561	65	404	117
33	920	861	95	586	176
34	445	457	65	317	92
35	670	641	84	490	103
36	685	798	110	719	187
37	741	739	94	665	153
38	387	406	56	257	95
39	515	563	78	522	131

40	611	692	87	497	149
41	589	639	37	386	112
42	459	504	32	335	111
43	898	970	54	920	175
44	570	657*	43	494	133
45	633	690	41	571	137
46	847	904	46	634	159
47	702	770	46	709	142
48	681	740	44	620	143
49	763	844	48	893	188
50	716	774	44	789	150
51	548	637*	40	545	120
52	359	390	23	164*	67
53	853	948	59	864	164
54	289	324	22	152*	67
55	779	818	43	539	135
56	46	55*	4	20*	13
Total	35,742	36,312	-	32,361	-
Average absolute estimation error (AAEE)	-	57	-	107	-
Average relative root mean squared error (ARRTMSE)	-	-	11%	-	28%
Estimated coverage rate	-	93%	-	93%	-

Notes: (1) $RTM\hat{SE}^I = \sqrt{M\hat{SE}(\hat{T}_m^I)}$, $I = HY, FH$ and the alternative estimator of \hat{e}_m in Step 4 is used for $M\hat{SE}(\hat{T}_m^{HY})$

(2) * denotes T_m is not within $\hat{T}_m^I \pm 1.96\sqrt{MSE(\hat{T}_m^I)}$, $I = HY, FH$

(3) $RRTM\hat{SE}^I = \sqrt{M\hat{SE}(\hat{T}_m^I) / \hat{T}_m^I}$, $I = HY, FH$

(4) Estimated coverage rate = (# of true counts within the 95% confidence interval) divided by 56. The coverage rate of 93% is not significantly different (95% confidence) from the nominal coverage rate of 95%.

Table 2: FH estimates based on different big data coverage

Small area	T_m	\hat{T}_m^{FH}	$RTM\hat{SE}^{FH}$	$\hat{T}_m^{FH(1)}$	$RTM\hat{SE}^{FH(1)}$	$\hat{T}_m^{FH(2)}$	$RTM\hat{SE}^{FH(2)}$
1	910	800	176	854	156	673	167
2	426	478	105	478	90	504	79
3	728	642	141	639*	133	529	132
4	1014	1029	216	1042	210	1147	202
5	839	635	127	666	109	570*	110
6	383	276	80	277	76	284	69
7	529	511	112	500	105	555	98
8	730	668	174	563	167	650	191
9	447	308	129	313	118	310	125
10	433	317	95	318	85	384	80
11	544	280*	134	309*	140	270	152
12	751	898	225	800	227	1032	199
13	1236	1046	272	976	262	1066	268
14	650	623	156	538	142	644	128
15	350	332	100	281	89	295	76
16	499	458	169	504	172	428	176
17	312	146	142	147	138	179	141
18	768	790	158	782	138	996	132
19	507	439	83	483	78	443	62
20	857	972	156	1019	156	1131	155
21	1026	1144	252	1304	250	1124	237
22	732	559	173	633	153	607	168
23	706	848	187	823	148	799	117
24	584	704	148	712	136	751	152
25	412	474	142	425	134	454	157
26	800	821	156	840	143	871	170
27	896	1098	253	1014	247	1209	249
28	794	594	226	598	226	639	218
29	391	294	82	312	82	320	73
30	607	502	95	508	87	519	66
31	632	583	128	632	131	526	116
32	543	404	117	386	112	400	103
33	920	586	176	551*	174	572*	143
34	445	317	92	325	82	290	99
35	670	490	103	491	97	527	90
36	685	719	187	773	190	663	188
37	741	665	153	602	147	485*	124
38	387	257	95	251	87	307	83
39	515	522	131	504	122	465	99
40	611	497	149	461	129	464	109

41	589	386	112	350*	106	347*	95
42	459	335	111	298	101	268	128
43	898	920	175	909	182	730	160
44	570	494	133	519	137	528	111
45	633	571	137	620	120	589	93
46	847	634	159	662	130	512*	120
47	702	709	142	729	131	771	111
48	681	620	143	688	127	485	107
49	763	893	188	901	181	847	156
50	716	789	150	804	140	827	156
51	548	545	120	497	116	657	102
52	359	164*	67	160*	65	202	60
53	853	864	164	838	169	847	147
54	289	152*	67	157*	62	153*	55
55	779	539	135	548	131	446*	100
56	46	20*	13	23	12	10*	11
Total	35,742	32,361	-	32,337		32,301	-
Average absolute estimation error (AAER)	-	107	-	109		139	-
Average relative root mean squared error (ARRTMSE)	-	-	28%	-	27%	-	26%
Estimated coverage rate	-	93%	-	89%	-	86%	-

Notes: (1) * denotes T_m is not within $\hat{T}_m^{FH} \pm 1.96\sqrt{M\hat{S}E(\hat{T}_m^{FH})}$ or $\hat{T}_m^{FH^{(i)}} \pm 1.96\sqrt{M\hat{S}E(\hat{T}_m^{FH^{(i)}})}$, $i=1,2$.

(2) The coverage rates of 93%, 89% and 86% are not significantly different (95% confidence) from the nominal coverage rate of 95%.

REFERENCES

- Abadie, A., & Imbens, G. W. (2008) On the failure of the bootstrap for matching estimators. *Econometrica*, **76**, 1537–1557.
- Australian Bureau of Statistics (2015). MADIP. Available at <https://www.abs.gov.au/about/data-services/data-integration/integrated-data/multi-agency-data-integration-project-madip>.
- Australian Bureau of Statistics (2020) Census of Population and Housing, 2016. Available at <https://www.abs.gov.au/statistics/microdata-tablebuilder/datalab>.
- Alfeilat, H., Hassanat, A., Lasassmeh, O., Tarawneh, A., Alhasanat, M., Salman, H. and Prasath, V. (2019) Effects of Distance Measure Choice on K-Nearest Neighbour Classifier Performance: A Review. *Big Data*, **7**, 221 -248.
- Amaya, A. Biemer, P. and Kinyon, D (2020) Total Error in a Big data World. Adapting the TSE Framework to Big Data. *Journal of Survey Statistics and Methodology*, **8**, 89-119.
- Beaumont, J.-F. (2005) Calibrated imputation in surveys under a quasi-model-assisted approach. *Journal of the Royal Statistical Society*, **B67**, 445 – 458.
- Beaumont, J.-F. (2020) Are probability surveys bound to disappear for the production of official statistics? *Survey Methodology*, **46**, 1 – 28.
- Callegaro, M. and DiSogra C. (2008). Computing Response Metrics for Online Panels. *Public Opinion Quarterly*, **72**, 1008–1032.
- Chipperfield, J., Chessman, J. and Lim, R. (2012) Combining household surveys using mass imputation to estimate population totals. *Australian & New Zealand Journal of Statistics*, **54**, 223– 238.
- Daas, P. J. H., Puts, M. J. and van den Hurk, P. A. M. (2015) Big data as a source for official statistics. *Journal of Official Statistics*, **31**, 249 – 262.
- Datta, G. S. (2009) Model-based approach to small area estimation. In *Sample Surveys: Inference and Analysis*, (D. Pfeiffermann and C. R. Rao, eds.). *Handbook of Statistics*, **29B**, 251–288. North-Holland, Amsterdam.
- Deville, J.-C. and Särndal, C.-E. (1992) Calibration estimators in survey sampling. *Journal of the American Statistical Association*, **87**, 376–382.
- Efron, B. and Gong, G. (1983) A leisurely look at the Bootstrap, the Jackknife and Cross Validation. *The American Statistician*, **37**, 36-48.
- Fay, R. and Herriot, R. (1979) Estimates of Income for Small Places: An Application of James-Stein Procedures to Census data. *Journal of the American Statistical Association*, **74**, 269 – 277.
- Fellegi, I. P. and Sunter, A. B. (1969). A theory for record linkage. *Journal of the American Statistical Association*, **40**, 1183 – 1210.

- Hobza, T. and Morales, D. (2016). Empirical best prediction under unit-level logit mixed models. *Journal of Official Statistics*, **32**, 661.
- Ghosh, M. and Rao, J.N.K. (1994) Small area estimation: An appraisal. *Statistical Science*, **9**, 55 – 93.
- Ghosh, M. (2020) Small area estimation: its evolution in five decades. *Statistics in Transition New Series*, New York, **Vol. 2, Issue 4**, 1-22,
- Hastie, T., Tibshirani, R. and Friedman, J. (2008) *The Elements of Statistical Learning: Data Mining, Inference and Prediction*. Second Edition: Springer.
- Hassanat, A.B. (2014) Dimensionality Invariant Similarity Measure. *Journal of American Science*, **10**, 221 -226.
- Jiang, J. and Lahiri, P. (2006a) Estimation of finite population domain means: A model-assisted empirical best prediction approach. *Journal of the American Statistical Association*, **101**, 301–311.
- Jiang, J. and Lahiri, P. (2006b) Mixed model prediction and small area estimation. *Test*, **15**, 1–96.
- Lehtonen, R. and Veijanen, A. (2009) Design-based methods of estimation for domains and small areas. In *Sample Surveys: Inference and Analysis* (D. Pfeffermann and C. R. Rao, eds.). *Handbook of Statistics*, **29B**, 219–249. North-Holland, Amsterdam
- Kim, J. K., Park, S., Chen, Y. and Wu, C. (2020) Combining non-probability and probability survey samples through mass imputation. *Journal of the Royal Statistical Society Series A*, **184**, 941 – 963.
- Kim, J.K. and Tam, S. M. (2021) Data integration by combining big data and survey sample data for finite population inference. *International Statistical Review*, **89**, 382-401
- Marchetti, S., Giusti, C., Pratesi, M., Salvati, N., Giannotti, F., Pedreschi, D., Rinzivillo, S., Pappalardo, L and Gabrielli, L. (2015) Small area model-based estimators using big data sources. *Journal of Official Statistics*, **31**, 263-281.
- Medious, E., Goga, C., Ruiz-Gazen, C., Beaumont, J. F., Dessertaine, A. and Puech, P. (2022). QR prediction for statistical data integration. Available at: <https://www.tse-fr.eu/publications/qr-prediction-statistical-data-integration>.
- Molina, I. and Marhuenda, Y. (2015). Sae: An R Package for Small Area Estimation. *The R Journal*, **7**, 81 – 98.
- Otsu, T., and Rai, Y. (2017) Bootstrap inference of matching estimators for average treatment effects. *Journal of the American Statistical Association*, **112**, 1720 – 1732.
- Pfeffermann, D. (2002) Small area estimation – New developments and directions. *International Statistical Review*, **70**, 125 – 143.
- Pfeffermann, D. (2013) New important developments in small area estimation. *Statistical Science*, **28**, 40- 68.
- Pfeffermann, D. and Tiller, R. (2006) Small area estimation with state-space models subject to benchmark constraints. *Journal of the American Statistical Association*, **101**, 1387-1397.

Podesta, J., Pritzker, P., Monitz, E., Holdren, J. & Zients, J. (2014). Big Data: Seizing opportunities, preserving values Washington: Executive Office of the President. Available at: http://www.whitehouse.gov/sites/default/files/docs/big_data_privacy_report_May_1_2014.pdf.

Porter, A. T., Holan, S. H., Wikle, C. K. and Cressie, N. (2014) Spatial Fay-Herriot model for small area estimation with functional covariates. *Spatial Statistics*, **10**, 27-42.

Rao, J. N. K. (2005) Inferential issues in small area estimation: Some new developments. *Statistics in Transition*, **7**, 513–526.

Rao, J. N. K. (2021) On Making Valid Inferences by Integrating Data from Surveys and Other Sources. *Sankhya Series*, **B83**, 242 – 272.

Rao, J. N. K. (2008). Some methods for small area estimation. *Revista Internazionale di Scienze Sociali*, **4**, 387–406.

Rao, J.N.K., and Molina, I. (2015) Small Area Estimation. Second Edition, Hoboken, New Jersey: John Wiley & Sons.

Särndal, C. E., Swensson, B. and Wretman, J. (1992). *Model Assisted Sampling*. Verlag, New York: Springer.

Schmid, T., Bruckschen, F., Salvati, N. and Zbiranski, T. (2017) Constructing sociodemographic indicators for national statistical institutes by using mobile phone data: estimating literacy rates in Senegal. *Journal of the Royal Statistical Society Series*, **A180**, 1163-1190.

Statistics New Zealand (2015). Integrated Data Infrastructure. <https://www.stats.govt.nz/integrated-data/integrated-data-infrastructure/>. Accessed 2 June, 2023.

Tam, S. M. and Clarke, F. (2015) Big data, official statistics and some initiative by the Australian Bureau of Statistics. *International Statistical Review*, **83**, 436 – 448.

Tam, S. M., Kim, J. K., Ang, and Pham, H. (2020). Mining the new oil for official statistics. In *Big Data Meets Survey Science: A Collection of Innovation Methods*, Hoboken, New York: John Wiley and Sons.

Tam, S. M. and van Halderen, G. (2020). The five V's, seven virtues and ten rules of engagement with big data. *Statistical Journal of the International Association for Official Statistics*, **36**, 423 -433..

Wikipedia (2022). Internet of Things. Available at https://en.wikipedia.org/wiki/Internet_of_things.

Yang, S. and Kim, J. K. (2020) Asymptotic theory and inference of predictive mean matching imputation using a superpopulation model framework. *Scandinavian Journal of Statistics*, **47**, 839 – 861.

Ybarra, L. M. R. and Lohr, S. (2008). Small area estimation when auxiliary information is measured with error. *Biometrika*, **95**, 919 – 931.

Yung, W., Tam, S. M., Buelens, B., Chipman, H., Dumpert, F., Ascari, G., Rocci, F., Burger, J. and Choi, I. (2021). A quality framework for statistical algorithms. *Statistical Journal of the International Association for Official Statistics*, **38**, 291 - 308.